Available online at www.sciencedirect.com
SCIENCE DIRECT®
Journal of Power Sources 114 (2003) 352–356
JOURNAL OF POWER SOURCES
www.elsevier.com/locate/jpowsour

Short communication

Investigation of $MmFe_2$ electrode for nickel–metal hydride battery applications

R. Muruganantham[a], N. Rajalakshmi[a,*], K.S. Dhathathreyan[a], Sundara Ramaprabhu[b]

[a]*Centre for Energy Research, SPIC Science Foundation, 64 Mount Road, Guindy, Chennai 600032, India*
[b]*Magnetism and Magnetic Materials Laboratory, Department of Physics, Indian Institute of Technology, Chennai 600036, India*

Received 6 August 2002; accepted 31 October 2002

Abstract

An electrochemical investigation is made on a Mischmetal–iron ($MmFe_2$) alloy for its suitability as an electrode for nickel–metal hydride (Ni–MH) batteries. Change–discharge characteristics, kinetics and life-cycle are studied. The charging capacity is around 350 mAh g^{-1}, which corresponds to a hydrogen concentration of 2.62 hydrogen atoms per formula unit and 25 activation cycles are required to attain the maximum capacity. Studies with the ac impedance method show that the kinetics are controlled by the charge-transfer mechanism. The $MmFe_2$ electrode can withstand prolonged charge–discharge with no deterioration in performance and high-rate capacity.

Keywords: Alloy; Battery; Charging capacity; Hydrogen storage; Nickel–metal hydride; Mischmetal

1. Introduction

Mischmetal (Mm)-based AB_2 Laves phase alloys have been considered as potential candidates for the negative electrode material in nickel–metal hydride (Ni–MH) batteries because of their higher electrochemical capacity, long life-cycle and relatively low cost [1–5]. The composition of Mischmetal depends on the source of the ore. The Mischmetal sample used in the present investigation is 99.5% pure and contains 30 wt.% La, 52 wt.% Ce, 13 wt.% Nd, and 5 wt.% Pr. Sakati et al. [6] reported that the decay in capacity of a MH electrode made of Mischmetal ($MmNi_{3.5}Co_{0.7}Al_{0.8}$) alloy was only 10% after 2000 cycles. As AB_2-type, multiphase, hydrogen-storage alloys are mainly composed of C_{14} and C_{15} Laves phase and some solid solutions with bcc structure, there exist abundant with enriched electrochemically catalytic elements as active reaction sites. Recently, we have reported the hydrogen-storage capacity, charge–discharge characteristics and diffusion coefficient for an AB_2 compound with the composition $Y_xZr_{(1-x)}Mn_mFe_nCo_pV_oCr_q$ ($m+n+o+p+q=2$), and have evaluated the processes that occur during charge and discharge [6]. It was found that an electrode made of zirconium-based alloys exhibited pulverization and deterioration properties with charge–discharge cycling. A Mm-based alloy shows much longer life-cycle and such alloys have a tendency to suffer less pulverization and deterioration properties with charge–discharge cycling. A Mm-based alloy shows much longer life-cycle and such alloys have a tendency to suffer less pulverization and deterioration on cycling. All these advantages are gained at much less cost. In the present paper, the electrochemical charging and discharging capacity, life-cycle and diffusion coefficient are studied for a $MmFe_2$ electrode, and the mechanism of hydrogen absorption is examined by ac impedance methods.

2. Experimental

A Mm-based alloy of composition $MmFe_2$ was prepared by arc melting Mischmetal with Fe in an argon atmosphere. The alloy was turned upside down and remelted five to six times in order to obtain good homogeneity. Alloy buttons were annealed at 900 K for about 48 h. The alloy was pulverized mechanically in an agate mortar. The structure and phase density were characterized by X-ray diffraction. The sample has an AB_2 phase. The electrodes were prepared

* Corresponding author. Tel.: +91-44-2301-726; fax: +91-44-235-1504.
E-mail address: cerssf@md5.vsnl.net.in (N. Rajalakshmi).

0378-7753/02/$ – see front matter
PII: S0378-7753(02)00612-2

by grinding the alloy down to 75 μm and mixed with copper powder in the ratio 1:3 with a PTFE binder. The putty form of the mixture was mechanically pressed on to a nickel mesh which acted as a current collector. The electrode was then sintered at 300 °C for about 3 h under vacuum. The electrochemical measurements were carried out in a glass apparatus with three compartments and flooded electrolyte condition in open cells. Potentials were monitored using a saturated calomel electrode (SCE) as reference electrode. The geometric area of the electrode was about 1.5 cm^2. The counter electrode was platinum, large, geometric area than the working electrode. The electrolyte, 30% KOH, was prepared

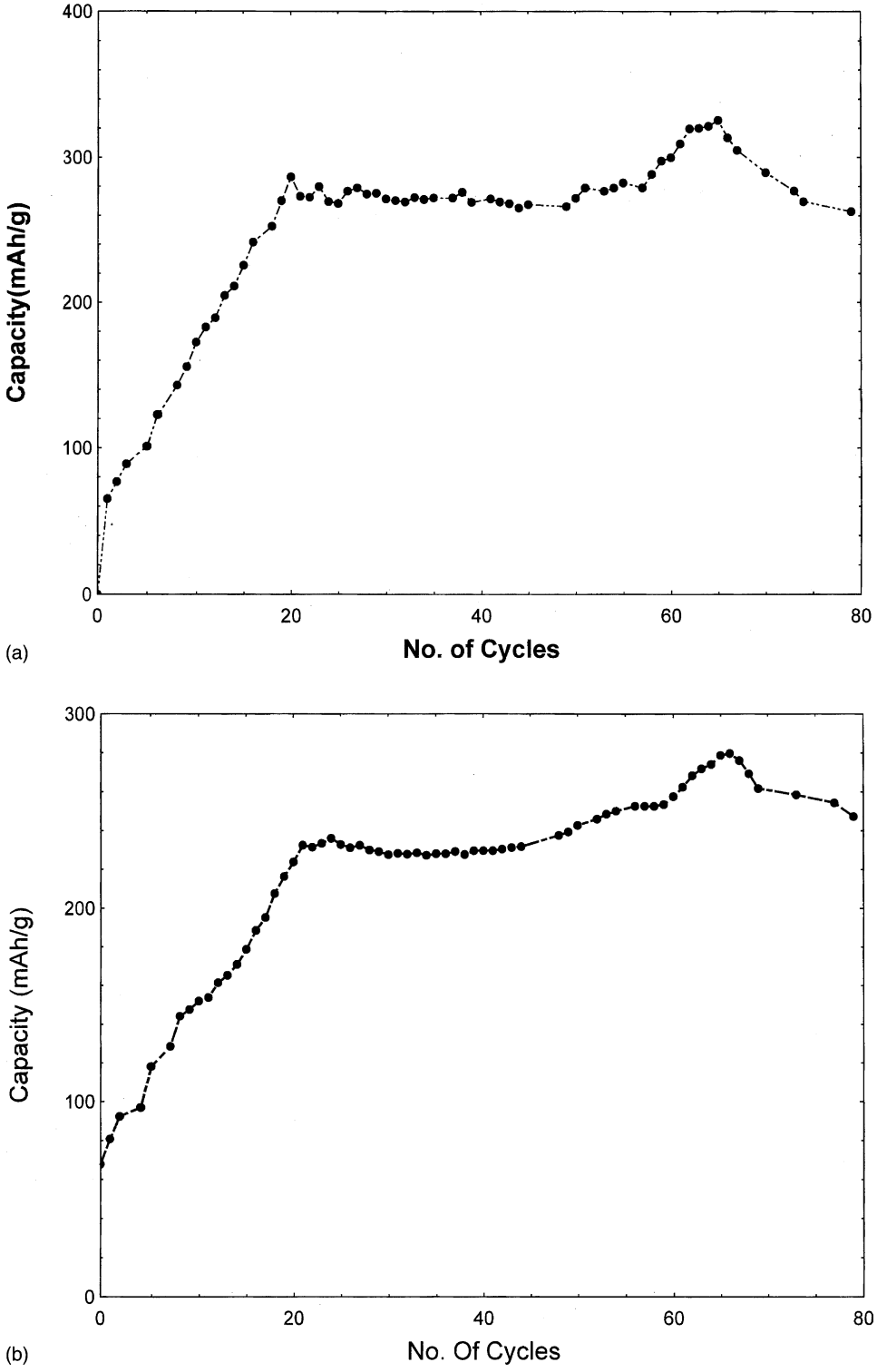

Fig. 1. Variation of (a) charging and (b) discharging capacity with life-cycle.

from reagent grade KOH and de-ionized water. The electrodes were tested for their charge–discharge characteristics, initial capacity, life-cycle, and kinetics. Electrochemical measurements were carried out by means of Voltalab PGZ 301 equipment.

3. Results and discussion

The electrochemical charge and discharge capacity of $MmFe_2$ alloy electrode as a function of cycle number are shown in Fig. 1(a) and (b), respectively. The charge capacity of the electrode reaches a maximum of 350 mAh g^{-1} after 25 cycles, which corresponds to 2.62 hydrogen atoms per formula unit, and remains at this value for almost 100 cycles, with a coulombic efficiency of 83%. Hydrogen evolution is found to occur at around −1.3 V, which shows that the metal hydride electrode is not extensively oxidized and, hence, can store hydrogen reversibly. The charge and discharge potential is around −0.7 and −0.4 V, respectively with respect to a SCE, as shown in Fig. 2. The degradation of the electrode also was found to be less than that of zirconium-based alloys. Generally, the decay in the capacity results from deterioration of the metal hydride electrode which is due to oxidation and pulverization of the alloy powder. It is considered that many of the grain boundaries in the metal hydride alloys have segregated layers, which are corroded in alkaline electrolyte. This results in an increase in electrode resistance which, in turn, decreases the hydrogen-absorbing capacity of the alloy. Since the capacity of the electrode remains constant even after repeated charging–discharging cycling, pulverization and oxidation are almost absent in the case of Mm-based alloys, and the electrodes are not corroded.

The value of the exchange current density reflects the rate of the charge-transfer reaction (i.e. hydrogen absorption and desorption) at the interface between the MH alloy powder and electrolyte. The exchange current density is dependent on both the activation of the MH alloy powder and the reaction surface area. In addition, the value of the exchange current density is influenced by the initial particle size, the construction of the MH electrode, and the additives in the electrode. An increase in exchange current density results in an increase in the high-rate discharge capability of the electrode.

With an increasing number of charge–discharge cycles, the MH alloy powders will crack and be pulverized into micron-sized particles because of hydrogen absorption and desorption. The cracks lead to an increase in the reaction surface and hence an improvement in activation for hydrogen adsorption at the electrode–electrotype interface.

It is known that the electrochemical hydriding and dehydriding processes of the hydrogen-storage alloy electrode in an alkaline solution include a charge-transfer step and a diffusion step. When charging, electrolytically generated hydrogen at the interface of the alloy and electrolyte diffuses into the bulk alloy and is stored in the metallic lattice in a hydride form. When discharging, the hydrogen stored in the bulk alloy moves towards the surface where it is oxidized.

The electrode reaction can be expressed as follows:

$$M + H_2O + e^- \rightarrow MH_{ads} + OH^- \quad (1)$$

$$MH_{ads} \rightarrow MH_{abs} \quad (2)$$

where H_{ads} and H_{abs} denote the hydrogen atoms on the surface of the MH alloy powder and in the bulk of the MH alloy, respectively. The electrochemical performance of the

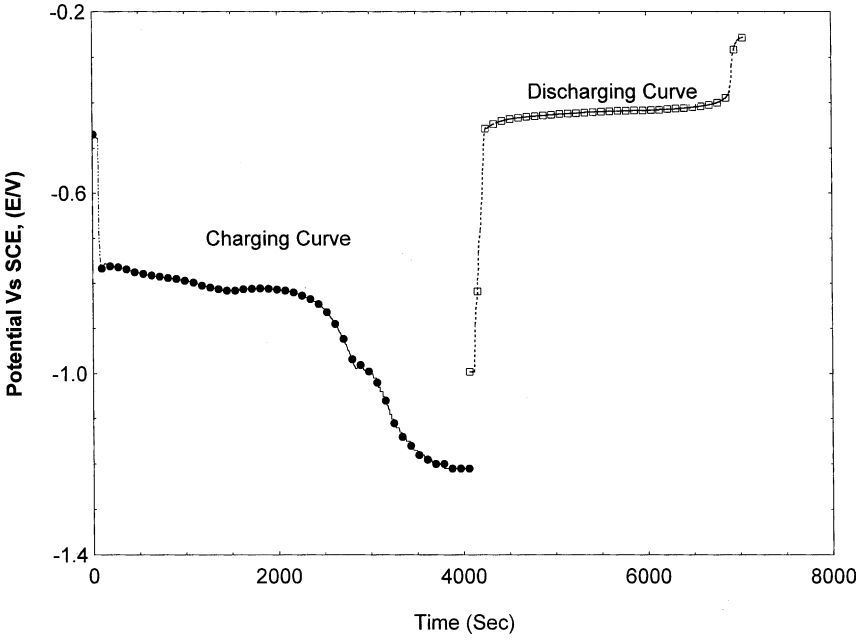

Fig. 2. Electrochemical charging and discharging of $MmFe_2$ electrode.

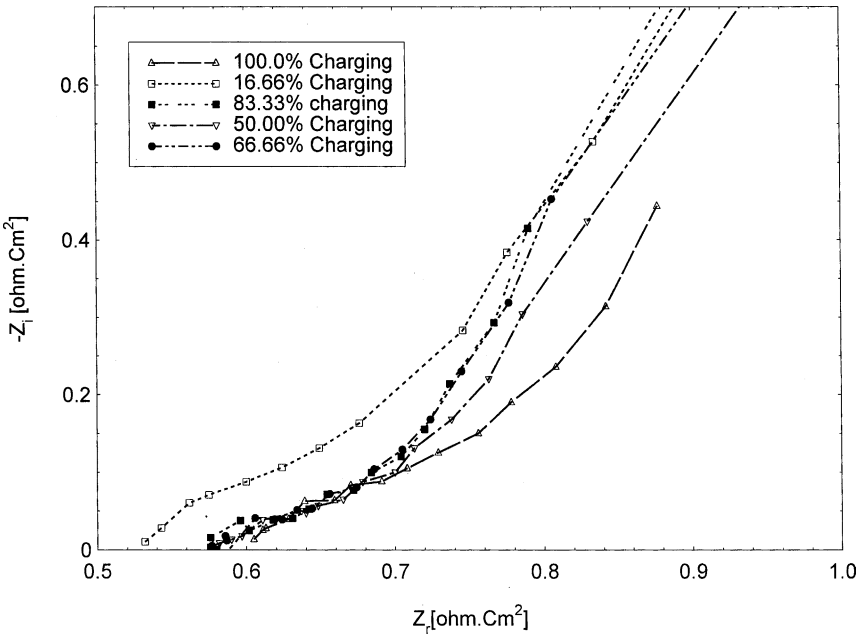

Fig. 3. Electrochemical impedance spectrum of $MmFe_2$ electrode.

hydriding and dehydriding reactions in alkaline solution is determined by the charge-transfer reaction at the alloy–electrolyte interface, i.e. Eq. (1), and the rate of hydrogen diffusion within the bulk of the alloy, i.e. Eq. (2).

In order to understand the mechanism of the electrochemical hydriding and dehydriding process, ac impedance spectra of the alloy electrodes were investigated for different charged states of hydrogen. The results are presented in Fig. 3. The electrochemical kinetics of the charge-transfer process were determined by the dc polarization curve which represent the electrode resistance (R_c). The electrode resistance is composed of the ohmic resistance (R_Ω) and the polarization resistance (R_p). The latter resistance is determined mainly by the charged-transfer process at the interface between the MH electrode and the electrolyte. This process can be described in terms of the exchange current density.

A semicircle at high frequencies and a slightly curved line at low frequencies were observed for a completely discharged electrode and a less charged electrode compared

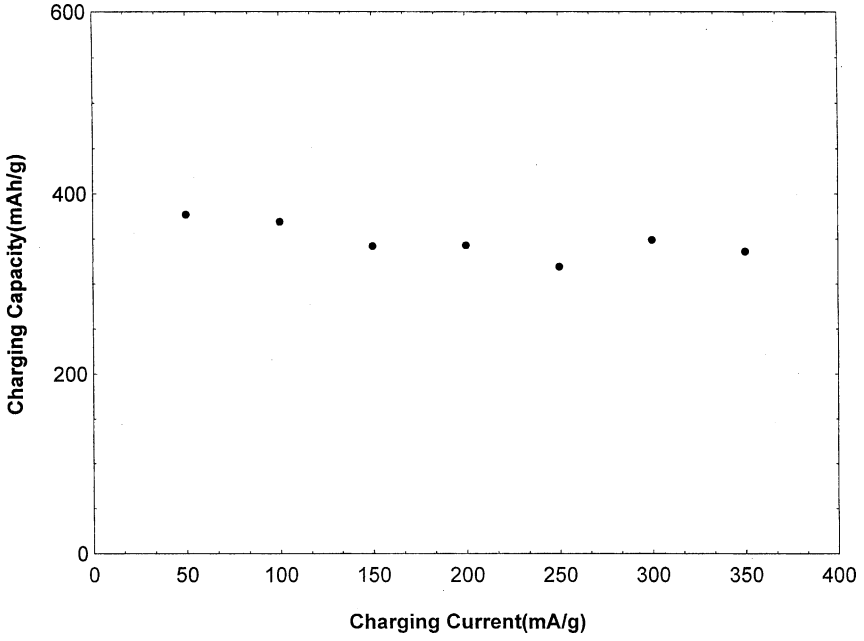

Fig. 4. Electrochemical charging capacity of $MmFe_2$ at various charging currents.

Table 1
Charge-transfer resistance (R_{ct}), polarization resistance (R_p) and exchange current density (i_0) at different states-of-charge (SoC)

SoC (%)	R_p (MΩ)	R_{ct} (MΩ)	i_0 (mA g^{-1})
16.66	537	672	18.5
50.00	560	706	18.0
66.66	553	664	22.5
83.33	580	689	22.9
100.00	606	704	25.5

with a completely charged electrode. The loop at high frequencies is characteristics of the charge-transfer process at the alloy–electrolyte interface, as shown by several authors [7,8]. The linear response at low frequencies is indicative of hydrogen diffusion in a bulk alloy [9]. The slight bending and slope deviation from 45° for the locus at low frequencies may be attributed to hydrogen diffusion in an alloy powder bulk and the pore geometry of a porous powder electrode [10]. The values of charge-transfer resistance R_{ct} calculated from the radius of semicircle at high frequencies for different states-of-charge (SoC) are given in Table 1, along with the polarization resistance and the exchange current density.

The exchange current density, i_0, a measure of the electrocatalytic nature of the modified alloy electrode [11–13], is calculated according to:

$$i_0 = \frac{RT}{nR_{ct}F} \tag{3}$$

where R is the gas constant, T the absolute temperature, n the number of transferred electrons and F the Faraday constant. The values in Table 1 show that the value of i_0, increases significantly on charging the sample. This indicates that the electrocatalytic activity on the surface of the alloy is greatly improved which, thereby, reduces the overpotential during the charge–discharge process. The capacity is lower when the electrodes are charged at 2 and 3 C rate, as shown in Fig. 4. The capacity decreases by about 30% when the charging current is increased from 50 to 350 mA g^{-1}. The highest electrochemical capacity is obtained after 25 cycles at the 1 C rate.

4. Conclusions

The hydrogen absorption capacity of a $MmFe_2$ electrode shows a charging capacity of 350 mA g^{-1}, which corresponds to a hydrogen concentration of 2.62 hydrogen atoms per formula unit. This capacity is comparable with that of zirconium-based AB_2 alloys, but the kinetics are slow. The exchange current density increases with state-of-charge, which reflects a fast hydrogen-absorption process at the interface between the metal hydride alloy powder and the electrolyte. Nickel–metal hydride batteries using Mischmetal as the negative electrode decreases the magnitude of the pulverization and deterioration of the alloy with charge–discharge cycling. Since the cost of both Mm and Fe are low, all these advantages are gained at much less cost.

Acknowledgements

The authors are grateful to the management, SPIC Science Foundation, for financial support and infrastructure facilities. One of the authors (SR) would like to thank CSIR, India for their financial support.

References

[1] T. Sakai, K. Oguro, H. Miyamura, N. Kuriama, A. Kato, H. Ishikawq, J. Less Common Met. 172–174 (1991) 1175.
[2] T. Sakai, A. Takagi, K. Kinoshita, N. Kuriama, H. Miyamura, H. Ishikawai, J. Less Common Met. 172–174 (1991) 1185.
[3] T. Sakai, A. Yuasa, H. Ishikawa, H. Miyamura, N. Kuriama, J. Less Cormnon Met. 172–174 (1991) 1194.
[4] T. Sakai, H. Yoshingana, H. Miyamura, N. Kuriama, H. Ishikawag, J. Alloys Comp. 180 (1992) 37.
[5] T. Sakai, K. Muta, H. Miyamura, N. Kuriama, H. Ishikawa, in: D.A. Corrigan, S. Srinivasan (Eds.), Proceedings of the Symposium on Hydrogen Storage Materials, Batteries and Electrochemistry, Electrochemical Society, vol. 59, 1992, pp. 92–95.
[6] T. Sakati, H. Yoshina, H. Migamura, N. Kurigama, H. Ishikawa, J. Alloys Compd. 180 (1992) 37;
(a) N. Rajalakshmi, K.S. Dhathathreyan, S. Ramaprabhu, Advances in Hydrogen Energy, Kluwer Academic Publisher, Dordrecht, 2000.
[7] N. Kuriyama, T. Sakai, H. Miyamura, I. Uehara, H. Ishikawa, T. Iwasaki, J. Alloys Compd. 202 (1993) 183.
[8] B.V. Ratnakumar, C. Witham, R.C. Bowman Jr., A. Hightower, B. Fultz, J. Electrochem. Soc. 143 (1996) 2578.
[9] N. Cui, B. Luan, H.K. Liu, X.X. Dou, J. Power Sources 63 (1996) 209.
[10] D.D. Mac Donald, R. Varma, J.R. Selman (Eds.), Wiley, New York, 1991.
[11] C. Iwakura, Y. Fumoto, M. Matsuoka, T. Zkohno, K. Shimnou, J. Alloys Compd. 192 (1993) 152.
[12] M. Matsuoka, M. Terashima, C. Iwakura, Electrochem. Acta 38 (1993) 1087.
[13] N. Cui, B. Luan, H.J. Zhao, H.K. Liu, S.X. Dou, J. Alloys Compd. 233 (1996) 236.